Theory uncertainties for Higgs mass and other searches using jet bins

Iain W. Stewart and Frank J. Tackmann

Phys. Rev. D **85**, 034011 — Published 7 February 2012

DOI: 10.1103/PhysRevD.85.034011

Theory Uncertainties for Higgs and Other Searches Using Jet Bins

Iain W. Stewart[1, 2] and Frank J. Tackmann[1]

[1] *Center for Theoretical Physics, Massachusetts Institute of Technology, Cambridge, MA 02139, USA*

[2] *Center for the Fundamental Laws of Nature, Harvard University, Cambridge, MA 02138, USA*

Bounds on the Higgs mass from the Tevatron and LHC are determined using exclusive jet bins to maximize sensitivity. Scale variation in exclusive fixed-order predictions underestimates the perturbative uncertainty for these cross sections, due to cancellations between the perturbative corrections leading to large K factors and those that induce logarithmic sensitivity to the jet-bin boundary. To account for this, we propose that scale variation in the fixed-order calculations should be used to determine theory uncertainties for inclusive jet cross sections, whose differences yield exclusive jet cross sections. This yields a theory correlation matrix for the jet bins such that the additional uncertainty from large logarithms due to the jet boundary cancels when neighboring bins are added. This procedure is tested for $H + 0, 1$ jets, $WW + 0$ jets, and $W + 0, 1, 2$ jets, and found to be generally applicable. For a case where the higher-order resummation of the jet boundary corrections is known, we show that this procedure yields fixed-order uncertainties which are theoretically consistent with those obtained in the resummed calculation.

I. INTRODUCTION

In the search for the Higgs boson at the Tevatron and the Large Hadron Collider (LHC), the data are divided into exclusive jet bins. This is done because the background composition depends on the number of jets in the final state, and the overall sensitivity can be increased significantly by optimizing the analysis for Higgs + 0, 1, and 2 jet signals. The primary example is the $H \to WW^*$ decay channel, which dominates the current Tevatron exclusion limits around $m_H \simeq 2m_W$ [1, 2], and is one of the important channels for $m_H \gtrsim 130\,\text{GeV}$ being pursued at the LHC [3, 4]. The importance of the Higgs + 1 jet channel in $H \to \tau\tau$ and $H \to WW^*$ was demonstrated explicitly in Refs. [5, 6]. Similarly, for $H \to \gamma\gamma$, which plays an important role for $m_H \lesssim 130\,\text{GeV}$, the search sensitivity can be improved by optimizing the analysis for different jet bins [7].

Since the measurements are performed in each jet bin, the perturbative uncertainties in the theoretical predictions must also be evaluated separately for each jet multiplicity [8]. Furthermore, to combine the results in the end, the correlations between the theoretical uncertainties in the different jet bins as well as in the total cross section have to be understood and taken into account.

In the winter 2011 Tevatron analyses of $gg \to H \to WW^*$ [2], the perturbative uncertainties in the signal cross section are evaluated using common scale variation for the exclusive jet bins, which yields [8]

$$\frac{\Delta\sigma_{\text{total}}}{\sigma_{\text{total}}} = 66.5\% \times \binom{+5\%}{-9\%} + 28.6\% \times \binom{+24\%}{-22\%} + 4.9\% \times \binom{+78\%}{-41\%} = \binom{+14\%}{-14\%}. \quad (1)$$

The three terms are the contributions from the 0, 1, and ($\geq$ 2)-jet bins with their relative scale uncertainties in brackets. By using a common scale variation the uncertainties are effectively 100% correlated and are added linearly, such that the $\pm 14\%$ scale uncertainty in the total cross section is reproduced.

For the 0-jet bin, which is the most sensitive search channel in $H \to WW^*$, one applies a strong veto on additional jets. It is often argued that with the jet veto the perturbative uncertainties improve, yielding scale uncertainties from fixed-order perturbation theory that are smaller than those in the total cross section, as seen in Eq. (1). This apparent improvement arises from cancellations between two sources, large corrections to the total cross section (large K factors) and the large corrections from logarithmic dependence on the jet veto. Since the improvement arises from a cancellation between two large and predominantly independent perturbative series, it must be assessed carefully.

We propose a simple procedure to estimate more realistic perturbative uncertainties for exclusive jet bins from fixed-order perturbation theory. The method is designed for processes with large K factors or large perturbative corrections in inclusive cross sections and takes into account the structure of the various perturbative series. As we will see, it can also be applied in general. The essential idea is to first independently determine the uncertainties in the inclusive N-jet cross sections $\sigma_{\geq N}$, and then use them to compute the uncertainty in the exclusive N-jet cross section σ_N from the difference

$$\sigma_N = \sigma_{\geq N} - \sigma_{\geq N+1}\,. \quad (2)$$

To a first approximation the perturbative series for $\sigma_{\geq N}$ can be considered unrelated for different N. For instance, their series start at different orders in α_s, and there is a priori no direct relation between the modifications to the series caused by the jet cuts that define these two inclusive samples. Therefore, as explained in detail in Sec. II, we can work in the limit where the fixed-order perturbative uncertainties in the $\sigma_{\geq N}$'s can be taken as uncorrelated, leading to

$$\Delta_N^2 = \Delta_{\geq N}^2 + \Delta_{\geq N+1}^2\,. \quad (3)$$

The uncertainty in the exclusive cross section is larger

than that in the corresponding inclusive one, which accounts for its more complicated perturbative structure. Equation (2) also leads to an anti-correlation between the cross sections in neighboring jet bins. When neighboring bins are added the sensitivity to the boundary between them cancels and the uncertainty reduces accordingly.

For example, for the 0-jet bin in $H \to WW^*$ discussed above, we have $\sigma_0 = \sigma_{\text{total}} - \sigma_{\geq 1}$. Here, $\sigma_{\geq 1}$ contains double logarithms of the jet p_T cut, whereas σ_{total} does not involve any jet definition, so their perturbative series can be considered largely independent. Therefore, taking their perturbative uncertainties Δ_{total} and $\Delta_{\geq 1}$ as uncorrelated, the covariance matrix for $\{\sigma_0, \sigma_{\geq 1}\}$ is[1]

$$\begin{pmatrix} \Delta^2_{\text{total}} + \Delta^2_{\geq 1} & -\Delta^2_{\geq 1} \\ -\Delta^2_{\geq 1} & \Delta^2_{\geq 1} \end{pmatrix} . \tag{4}$$

Using this matrix to compute the uncertainty in $\sigma_0 + \sigma_{\geq 1}$ reproduces Δ_{total} as it should.

We should mention that we are only discussing here the uncertainties due to unknown higher-order perturbative corrections, which are commonly estimated using scale variations. We do not discuss parametric uncertainties, such as PDF and α_s uncertainties, which have been extensively discussed, recently for example in Refs. [9–16].

In the next section we present the arguments leading to our proposal for evaluating the perturbative uncertainties for exclusive jet bins, and discuss the structure of the perturbative series. In Sec. III, we apply our method to a variety of processes. We start in Secs. III A and III B with discussion and numerical results for $gg \to H + 0$ jets and $gg \to H + 1$ jets. In Sec. III C, we consider $pp \to WW + 0$ jets, which is an important background for Higgs production. In Secs. III D, III E, and III F we consider $W + 0, 1, 2$ jets, which are important backgrounds for missing-energy searches. In Sec. IV, we consider again $gg \to H + 0$ jets and test our method for the fixed-order uncertainties against a case where the resummation of the large logarithms induced by the jet binning is known to next-to-next-to-leading logarithmic (NNLL) accuracy. We conclude in Sec. V. In App. A, we give expressions for the uncertainties and correlations for the case where one considers 0, 1, and (≥ 2)-jet bins as in Eq. (1).

II. JET BIN UNCERTAINTIES

To examine in more detail the modification of the perturbative series that takes place for exclusive jet bins, we will consider the example of the 0-jet bin and (≥ 1)-jet bin. The total cross section, σ_{total}, is divided into a 0-jet exclusive cross section, $\sigma_0(p^{\text{cut}})$, and the (≥ 1)-jet inclusive cross section, $\sigma_{\geq 1}(p^{\text{cut}})$,

$$\begin{aligned} \sigma_{\text{total}} &= \int_0^{p^{\text{cut}}} \mathrm{d}p \, \frac{\mathrm{d}\sigma}{\mathrm{d}p} + \int_{p^{\text{cut}}} \mathrm{d}p \, \frac{\mathrm{d}\sigma}{\mathrm{d}p} \\ &\equiv \sigma_0(p^{\text{cut}}) + \sigma_{\geq 1}(p^{\text{cut}}) \, . \end{aligned} \tag{5}$$

Here, p denotes the kinematic variable which is used to divide the cross section into jet bins. For most of our analysis we take $p \equiv p_T^{\text{jet}}$, which for Eq. (5) is the largest p_T of any jet in the event. In this case, $\sigma_0(p_T^{\text{cut}})$ only contains events with jets having $p_T \leq p_T^{\text{cut}}$, and $\sigma_{\geq 1}(p_T^{\text{cut}})$ contains events with at least one jet with $p_T \geq p_T^{\text{cut}}$.

In Eq. (5) both σ_0 and $\sigma_{\geq 1}$ depend on the phase space cut, p^{cut}, and by construction this dependence cancels in their sum. This means that the additional perturbative uncertainty induced by this cut, call it Δ_{cut}, must be 100% anti-correlated between $\sigma_0(p^{\text{cut}})$ and $\sigma_{\geq 1}(p^{\text{cut}})$. That is, the contribution of Δ_{cut} to the covariance matrix for $\{\sigma_0, \sigma_{\geq 1}\}$ must be of the form

$$C_{\text{cut}} = \begin{pmatrix} \Delta^2_{\text{cut}} & -\Delta^2_{\text{cut}} \\ -\Delta^2_{\text{cut}} & \Delta^2_{\text{cut}} \end{pmatrix} . \tag{6}$$

The questions then are: (1) How can we estimate Δ_{cut}, and (2) how is the overall perturbative uncertainty Δ_{total} of σ_{total} related to the uncertainty for σ_0 and $\sigma_{\geq 1}$.

To answer these questions, we discuss the perturbative structure of the cross sections in more detail. By restricting the cross section to the 0-jet region, one restricts the collinear initial-state radiation from the colliding hard partons as well as the overall soft radiation in the event. This restriction on additional emissions leads to the appearance of Sudakov double logarithms of the form $L^2 = \ln^2(p^{\text{cut}}/Q)$ at each order in a perturbative expansion in the strong coupling constant α_s, where Q is the hard scale of the process. For Higgs production from gluon fusion, $Q = m_H$, and the leading double logarithms appearing at $\mathcal{O}(\alpha_s)$ are

$$\sigma_0(p_T^{\text{cut}}) = \sigma_B \Big(1 - \frac{3\alpha_s}{\pi} \, 2 \ln^2 \frac{p_T^{\text{cut}}}{m_H} + \cdots \Big) , \tag{7}$$

where σ_B is the Born (tree-level) cross section.

The total cross section just depends on the hard scale Q, which means by choosing the scale $\mu \simeq Q$, the fixed-order expansion does not contain large logarithms and has the structure[2]

$$\sigma_{\text{total}} \simeq \sigma_B \big[1 + \alpha_s + \alpha_s^2 + \mathcal{O}(\alpha_s^3) \big] . \tag{8}$$

[1] Since these are theory uncertainties, there is no strict reason to combine them in a particular way. We add them in quadrature since this is the most convenient for discussing correlations and error propagation.

[2] These expressions for the perturbative series are schematic. They do not show the convolution with the parton distribution functions (PDFs) contained in σ_B, nor do they display μ dependent logarithms. In particular, the single logarithms related to the PDF evolution are not displayed, since they are not the logarithms we are most interested in discussing.

The coefficients of this series can be large, corresponding to the well-known large K factors. For instance, the cross section for $gg \to H$ doubles from leading order to next-to-leading order (NLO) even though $\alpha_s \sim 0.1$. As usual, varying the scale in α_s (and the PDFs) one obtains an estimate of the size of the missing higher-order terms in this series, corresponding to Δ_{total}.

The inclusive 1-jet cross section has the perturbative structure

$$\sigma_{\geq 1}(p^{\text{cut}}) \simeq \sigma_B \big[\alpha_s(L^2+L+1) + \alpha_s^2(L^4+L^3+L^2+L+1) + \mathcal{O}(\alpha_s^3 L^6)\big] , \tag{9}$$

where the logarithms $L = \ln(p^{\text{cut}}/Q)$ arise from cutting off the IR divergences in the real emission diagrams. For $p^{\text{cut}} \ll Q$ the logarithms can get large enough to overcome the α_s suppression. In the limit $\alpha_s L^2 \simeq 1$, the fixed-order perturbative expansion breaks down and the logarithmic terms must be resummed to all orders in α_s to obtain a meaningful result. For typical experimental values of p^{cut} fixed-order perturbation theory can still be considered, but the logarithms cause large corrections at each order and dominate the series. This means varying the scale in α_s in Eq. (9) directly tracks the size of the large logarithms and therefore allows one to get some estimate of the size of missing higher-order terms caused by p^{cut}, that correspond to Δ_{cut}. Therefore, we can approximate $\Delta_{\text{cut}} = \Delta_{\geq 1}$, where $\Delta_{\geq 1}$ is obtained from the scale variation for $\sigma_{\geq 1}$.

The exclusive 0-jet cross section is equal to the difference between Eqs. (8) and (9), and so has the schematic structure

$$\sigma_0(p^{\text{cut}}) \simeq \sigma_B \Big\{ \big[1+\alpha_s+\alpha_s^2+\mathcal{O}(\alpha_s^3)\big] - \big[\alpha_s(L^2+L+1) + \alpha_s^2(L^4+L^3+L^2+L+1) + \mathcal{O}(\alpha_s^3 L^6)\big] \Big\} . \tag{10}$$

In this difference, the large positive corrections in σ_{total} partly cancel against the large negative logarithmic corrections. For example, at $\mathcal{O}(\alpha_s)$ there is a value of L for which the α_s terms in the schematic Eq. (10) cancel exactly, indicating that at this p^{cut} the NLO cross section has vanishing scale dependence and is equal to the LO cross section, $\sigma_0(p^{\text{cut}}) = \sigma_B$. We will see this effect explicitly in our examples below, using the complete perturbative expressions. We will find that this occurs for values of p^{cut} in the experimentally relevant region. Due to this cancellation, a standard use of scale variation in Eq. (10) does not actually probe the size of the logarithms, and thus is not suitable to estimate Δ_{cut}.

Since Δ_{cut} and Δ_{total} are by definition uncorrelated, by associating $\Delta_{\text{cut}} = \Delta_{\geq 1}$ we are effectively treating the perturbative series for σ_{total} and $\sigma_{\geq 1}$ as independent with separate (uncorrelated) perturbative uncertainties. That is, considering $\{\sigma_{\text{total}}, \sigma_{\geq 1}\}$, the covariance matrix is diagonal,

$$\begin{pmatrix} \Delta^2_{\text{total}} & 0 \\ 0 & \Delta^2_{\geq 1} \end{pmatrix} . \tag{11}$$

This is consistent, since for small p^{cut} the two series have very different structures. In particular, there is no reason to believe that the same cancellations in σ_0 will persist at every order in perturbation theory at a given p^{cut}.

From Eq. (11) it follows that the perturbative uncertainty in $\sigma_0(p^{\text{cut}})$ is given by $\Delta^2_{\text{total}} + \Delta^2_{\geq 1}$, i.e., by summing the inclusive cross section uncertainties in quadrature. It also follows that the complete covariance matrix for the three[3] quantities $\{\sigma_{\text{total}}, \sigma_0, \sigma_{\geq 1}\}$ is

$$C = \begin{pmatrix} \Delta^2_{\text{total}} & \Delta^2_{\text{total}} & 0 \\ \Delta^2_{\text{total}} & \Delta^2_{\geq 1} + \Delta^2_{\text{total}} & -\Delta^2_{\geq 1} \\ 0 & -\Delta^2_{\geq 1} & \Delta^2_{\geq 1} \end{pmatrix} , \tag{12}$$

where Δ_{total} and $\Delta_{\geq 1}$ are considered uncorrelated and are evaluated by separately varying the scales in the fixed-order predictions for σ_{total} and $\sigma_{\geq 1}(p^{\text{cut}})$, respectively. The $\Delta_{\geq 1}$ contributions in the lower right 2×2 matrix for σ_0 and $\sigma_{\geq 1}$ are equivalent to Eq. (6) with $\Delta_{\text{cut}} = \Delta_{\geq 1}$. Note that in this 2×2 space all of Δ_{total} occurs in the uncertainty for σ_0. This is reasonable from the point of view that σ_0 starts at the same order in α_s as σ_{total} and contains the same leading virtual corrections.

The limit $\Delta_{\text{cut}} = \Delta_{\geq 1}$ which Eq. (12) is based on is of course not exact but an approximation. However, the preceding arguments show that it is a more reasonable starting point than using a common scale variation for the different jet bins. The latter usually results in the cross sections being 100% correlated, as in Eq. (1), and in particular does not account for the additional p^{cut} induced uncertainties. In our numerical examples below, we will see that our method produces more sensible uncertainty estimates for fixed-order predictions. In Sec. IV we will compare the estimates from our method with those obtained by an explicit resummation in the jet-veto variable. This provides further evidence that our method gives consistent uncertainty estimates. Resummation provides a way for improving predictions for the central value of the cross section, together with better estimates of Δ_{cut} and the structure of the theory correlation matrix, as discussed in Sec. IV.

It is straightforward to generalize the above discussion to jet bins with more jets. For the N-jet bin we replace $\sigma_{\text{total}} \to \sigma_{\geq N}$, $\sigma_0 \to \sigma_N$, and $\sigma_{\geq 1} \to \sigma_{\geq N+1}$, and take the appropriate σ_B. If the perturbative series for $\sigma_{\geq N}$ exhibits large α_s corrections, then the additional large logarithms present in $\sigma_{\geq N+1}$ will again lead to cancellations

[3] The fact that only two of three are independent is reflected in the matrix, i.e. any 2×2 submatrix can be used to derive the full 3×3 matrix using the relation $\sigma_{\text{total}} = \sigma_0 + \sigma_{\geq 1}$.

when we consider the difference $\sigma_N = \sigma_{\geq N} - \sigma_{\geq N+1}$. Hence, $\Delta_{\geq N+1}$ will again give a better estimate for the $\Delta_{\rm cut}$ that arises from separating $\sigma_{\geq N}$ into jet bins σ_N and $\sigma_{\geq N+1}$. Another advantage of our procedure is that it is easily generalized to more than two jet bins by iteration. The case of three jet bins is given in App. A.

III. EXAMPLE PROCESSES

To elucidate the effect of $p_T^{\rm jet}$ vetoes on the fixed-order cross sections and demonstrate our method, we will now go through several explicit examples, considering in turn $H+0$ jets, $H+1$ jet, $WW+0$ jets, and $W+0$, 1, and 2 jets. All of our NLO p_T spectra are obtained using the MCFM code [17–20]. As our jet algorithm we use anti-k_T for the LHC results and a cone algorithm for the Tevatron results with $R = 0.5$ for both.

A. Higgs + 0 Jets

In Higgs production via gluon fusion the cross section is known to next-to-next-to-leading order (NNLO) [21–28], and exhibits large perturbative corrections. Consider the numerical results for the Higgs production cross section for $m_H = 165\,\text{GeV}$, $\mu_f = \mu_r = m_H/2$, and MSTW2008 NNLO PDFs [29], for which $\alpha_s \equiv \alpha_s(m_H/2) = 0.1189$. Here one finds [30–33]

$$\sigma_{\rm total} = (3.32\,\text{pb})\big[1 + 9.5\,\alpha_s + 35\,\alpha_s^2 + \mathcal{O}(\alpha_s^3)\big]\,, \quad (13)$$

for the LHC at $E_{\rm cm} = 7\,\text{TeV}$. Note that there is an α_s^2 in the Born cross section, $\sigma_B = 3.32\,\text{pb}$, but only the relative size of the corrections is important for our discussion. For the Tevatron the series is

$$\sigma_{\rm total} = (0.15\,\text{pb})\big[1 + 9.0\,\alpha_s + 34\,\alpha_s^2 + \mathcal{O}(\alpha_s^3)\big]\,. \quad (14)$$

In both cases the large K factors are clearly visible.[4] For the inclusive 1-jet cross section at the LHC one finds

$$\begin{aligned}\sigma_{\geq 1}&\big(p_T^{\rm jet} \geq 30\,\text{GeV}, |\eta^{\rm jet}| \leq 3.0\big)\\ &= (3.32\,\text{pb})\big[4.7\,\alpha_s + 26\,\alpha_s^2 + \mathcal{O}(\alpha_s^3)\big]\,,\\ \sigma_{\geq 1}&\big(p_T^{\rm jet} \geq 25\,\text{GeV}\big)\\ &= (3.32\,\text{pb})\big[6.0\,\alpha_s + 32\,\alpha_s^2 + \mathcal{O}(\alpha_s^3)\big]\,. \quad (15)\end{aligned}$$

The first values correspond to the ATLAS and CMS reference cuts, and the second to current ATLAS and CMS $H \to WW^*$ analyses [3, 4]. Similarly, for the typical cuts used in $H \to WW^*$ at the Tevatron [2], one finds

$$\begin{aligned}\sigma_{\geq 1}&\big(p_T^{\rm jet} \geq 20\,\text{GeV}, |\eta^{\rm jet}| \leq 2.5\big)\\ &= (0.15\,\text{pb})\big[4.1\,\alpha_s + 27\,\alpha_s^2 + \mathcal{O}(\alpha_s^3)\big]\,. \quad (16)\end{aligned}$$

In both Eqs. (15) and (16) one clearly sees the impact of the large logarithms on the perturbative series. Comparing to Eqs. (13) and (14) one also sees the sizeable numerical cancellation between the two series at each order in α_s. The extent of this cancellation depends sensitively on the value of $p^{\rm cut}$.

The perturbative uncertainties on these inclusive cross sections can now be used to determine the exclusive cross section uncertainties. Varying the scale up and down by a factor of two around $m_H/2$ gives for the Tevatron $\sigma_{\rm total} = (0.386 \pm 0.040)\,\text{pb}$ and $\sigma_{\geq 1} = (0.132 \pm 0.034)\,\text{pb}$ with the $p_T^{\rm jet}$ and $\eta^{\rm jet}$ cuts as in Eq. (16). Adding these in quadrature according to the upper-left entry in Eq. (4) gives

$$\sigma_0 = (0.254 \pm 0.052)\,\text{pb}\,, \quad (17)$$

i.e., a 20% uncertainty. In contrast, when doing a scale variation directly in the fixed-order expansion for $\sigma_0(p^{\rm cut})$, as in Eq. (1), one implicitly assumes that the perturbative uncertainties between the series for $\sigma_{\rm total}$ and $\sigma_{\geq 1}$ are 100% correlated, giving $\sigma_0 = (0.254 \pm 0.006)$. Here this leads to an underestimate for the remaining uncertainty. For the LHC, using the reference cuts, we get $\sigma_{\rm total} = (8.70 \pm 0.75)\,\text{pb}$ and $\sigma_{\geq 1} = (3.08 \pm 0.59)\,\text{pb}$, leading to

$$\sigma_0 = (5.63 \pm 0.96)\,\text{pb}\,, \quad (18)$$

i.e., a 17% uncertainty. In contrast, the direct scale variation for σ_0 yields $\sigma_0 = (5.63 \pm 0.15)$, which is again an underestimate.

The two procedures of evaluating uncertainties can be compared as a function of $p_T^{\rm cut}$, and in the upper left panel of Fig. 1 we do so for $\sigma_0(p_T^{\rm cut})$ for Higgs production. Results for σ_0 are obtained at NNLO for the LHC at $E_{\rm cm} = 7\,\text{TeV}$, using MCFM to calculate the $p_T^{\rm cut}$ dependence, FEHiP [30, 31] for the total NNLO cross section, and $\mu = m_H/2$ for central values. The central value is the solid blue curve, and the green dashed and dotted lines show the results of direct exclusive scale variation by a factor of two. For small values of $p_T^{\rm cut}$ the cancellations that take place for $\sigma_0(p^{\rm cut})$ cause the error bands to shrink. In particular, the direct exclusive scale uncertainty vanishes at $p_T^{\rm cut} \simeq 25\,\text{GeV}$, where there is an almost exact cancellation between the two series in Eq. (10), and the uncertainty curves pinch together. In contrast, the outer red solid lines show the result of our method, which combines the independent inclusive uncertainties to obtain the exclusive uncertainty,

[4] Using instead $\mu_f = \mu_r = m_H$ the coefficients of the α_s and α_s^2 terms increase to 11 and 65 for the LHC and 12 and 74 for the Tevatron, respectively. The α_s coefficients for the Tevatron for example arise as $9.0 = 4.9 + 2.0 + 2.1$ ($\mu = m_H/2$) and $12.0 = 4.9{+}5.7{+}1.4$ ($\mu = m_H$) where the three contributions are respectively from the terms in the partonic cross section proportional to $\delta(1-z)$, terms involving the plus functions $[1/(1-z)]_+$ and $[\ln(1-z)/(1-z)]_+$, and the remaining terms that are nonsingular for $z \to 1$. When separating these different terms we keep the overall $1/z$ factor in the convolution integral with measure $\mathrm{d}z/z$.

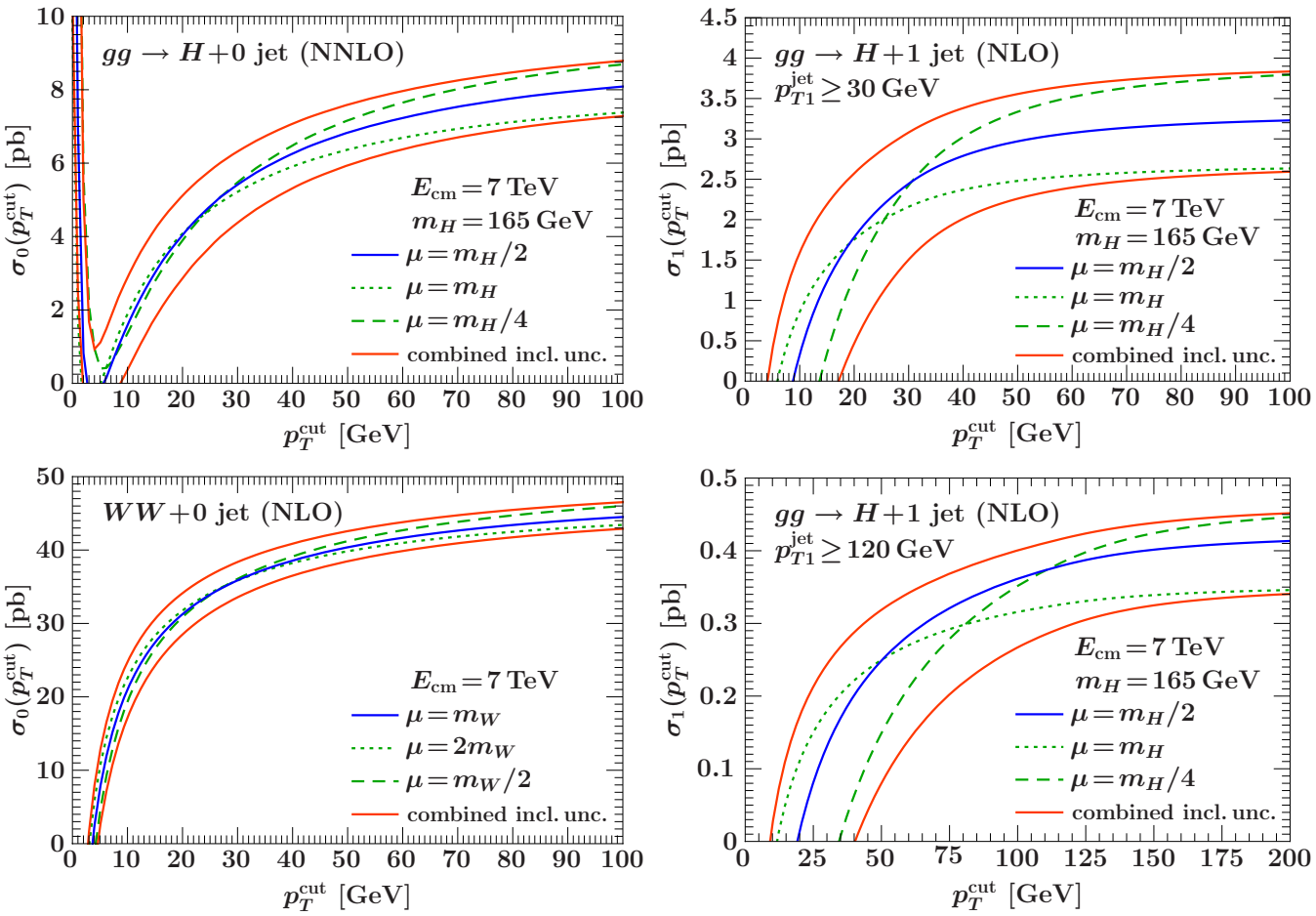

FIG. 1: Perturbative predictions for $H+0$ jets (upper left panel), $WW+0$ jets (lower left panel), $H+1$ jet with $p_{T1}^{\rm jet} \geq 30\,{\rm GeV}$ (upper right panel), and $H+1$ jet with $p_{T1}^{\rm jet} \geq 120\,{\rm GeV}$ (lower right panel). Central values are shown by the blue solid curves, direct scale variation in the exclusive jet bin by the green dashed and dotted curves, and the result of combining independent inclusive uncertainties to get the jet-bin uncertainty by the outer red solid curves.

$\Delta_0^2 = \Delta_{\rm total}^2 + \Delta_{\geq 1}^2$. One can see that for large values of $p_T^{\rm cut}$ this combined inclusive uncertainty estimate reproduces the direct exclusive scale variation, since $\sigma_{\geq 1}(p^{\rm cut})$ becomes small. On the other hand, for small values of $p_T^{\rm cut}$ the uncertainties obtained in this way are now more realistic, because they explicitly take into account the large logarithmic corrections. The features of this plot are quite generic. In particular, the same pattern of uncertainties is observed for the Tevatron, when we take $\mu = m_H$ as our central curve with $\mu = 2m_H$ and $\mu = m_H/2$ for the range of scale variation, and whether or not we only look at jets at central rapidities. We also note that using independent variations for μ_f and μ_r does not change this picture, in particular the μ_f variation for fixed μ_r is quite small.

Since both NLO and NNLO results for $\sigma_0(p_T^{\rm cut})$ are available, it is also useful to consider the convergence, which we show in Fig. 2 for the Tevatron (top row) and the LHC at 7 TeV (bottom row). In the left panels we directly vary the scales in $\sigma_0(p_T^{\rm cut})$ to estimate the uncertainty, while in the right panels we again propagate the uncertainties from the inclusive cross sections. As we lower $p_T^{\rm cut}$, the direct exclusive scale variation uncertainty estimate decreases at both NLO and NNLO, and eventually becomes very small when the curves pinch and the uncertainty is clearly underestimated. In contrast, the combined inclusive scale variation gives realistic uncertainties for all values of $p_T^{\rm cut}$. In particular, there is considerable uncertainty for small $p_T^{\rm cut}$ where the summation of logarithms is important.

B. Higgs + 1 Jet

As our next example we consider the 1-jet bin in Higgs production from gluon fusion. This jet bin is defined by two cuts, one which ensures that the jet with the largest p_T is outside the 0-jet bin, $p_{T1}^{\rm jet} \geq p_{T1}^{\rm cut}$, and one which ensures that the jet with the next largest p_T is restricted, $p_{T2}^{\rm jet} \leq p_T^{\rm cut}$, so that we do not have 2 or more jets. The 1-jet cross section can be computed as a difference of

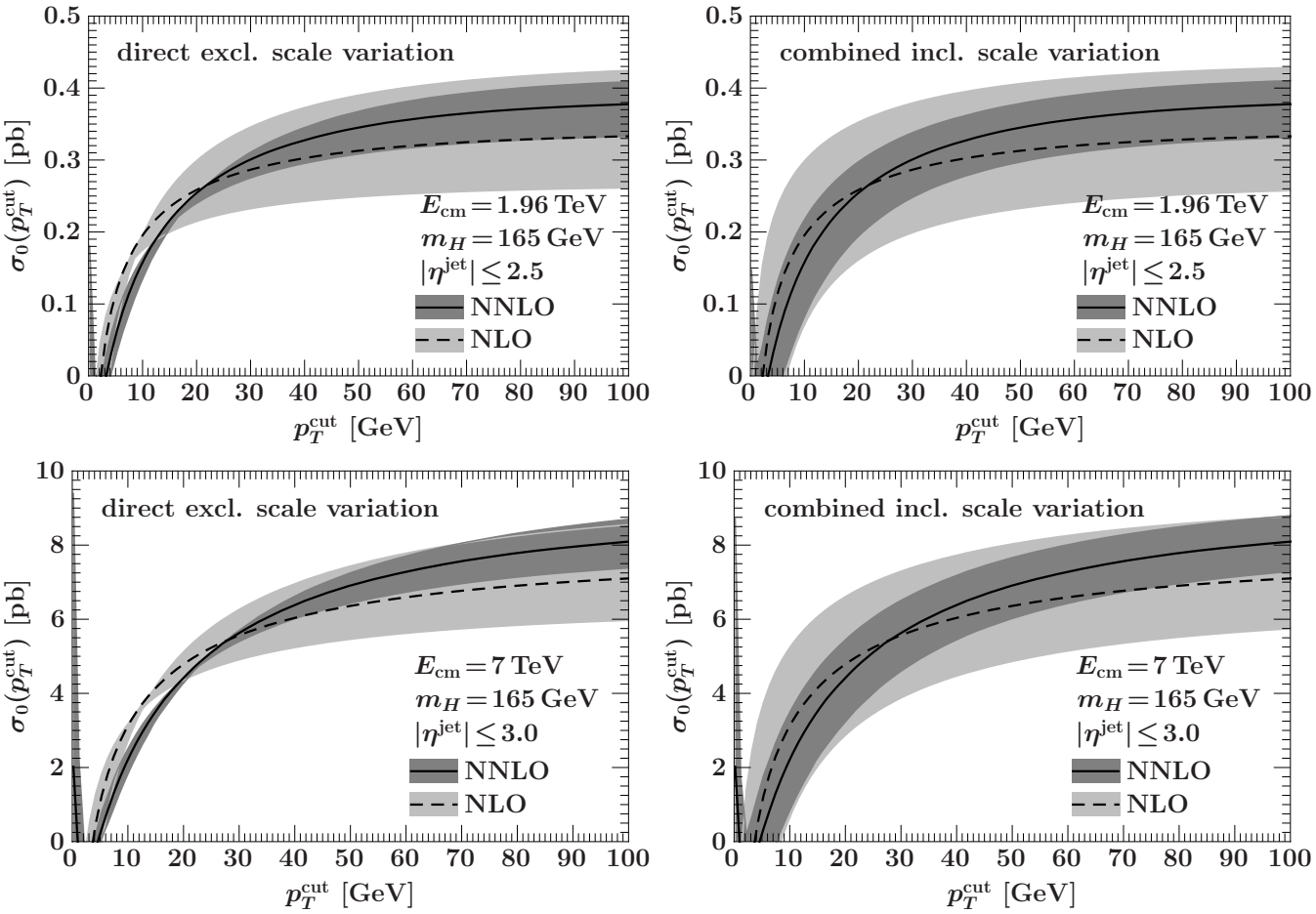

FIG. 2: Fixed-order perturbative uncertainties for $gg \to H + 0$ jets at NLO and NNLO. The upper row is for the Tevatron and the lower row for the LHC with $E_{\rm cm} = 7\,\text{TeV}$. On the left, the uncertainties are obtained from the direct scale variation in $\sigma_0(p_T^{\rm cut})$ between $\mu = m_H/4$ and $\mu = m_H$. On the right, the uncertainties are obtained by independently evaluating the scale uncertainties in $\sigma_{\rm total}$ and $\sigma_{\ge 1}(p^{\rm cut})$ and combining them in quadrature. (For the LHC case the dark shaded NNLO bands correspond to results in the top-left panel of Fig. 1. The direct exclusive scale variation band corresponds to the dashed green lines, and the combined inclusive uncertainty band corresponds to the solid red lines.)

inclusive cross sections with these cuts,

$$\sigma_1 = \sigma_{\ge 1}\big(p_{T1}^{\rm jet} \ge p_{T1}^{\rm cut}\big) - \sigma_{\ge 2}\big(p_{T1}^{\rm jet} \ge p_{T1}^{\rm cut}, p_{T2}^{\rm jet} \ge p_T^{\rm cut}\big)\,. \tag{19}$$

For convenience we adopt the notation that $p_T^{\rm cut}$ is always used for the cutoff that determines the upper boundary of the jet bin under consideration, which gives the analog of the L dependent terms in Eq. (10).

The inclusive cross section $\sigma_{\ge 1}$ that includes the 1-jet bin exhibits large perturbative corrections, much as $\sigma_{\rm total}$ does for the 0-jet bin. For $\sigma_{\ge 1}$ the large corrections are caused in part by the large double logarithmic series in $\ln(p_{T1}^{\rm jet}/m_H)$, but remains predominantly independent of the large double logarithms of $L = \ln(p_{T2}^{\rm jet}/m_H)$ which control the series for $\sigma_{\ge 2}$. With $\mu_f = \mu_r = m_H/2$, $m_H = 165\,\text{GeV}$, and MSTW2008 NNLO PDFs, we find

$$\begin{aligned}&\sigma_{\ge 1}\big(p_{T1}^{\rm jet} \ge 30\,\text{GeV}\big)\\ &\quad = (2.00\,\text{pb})\big[1 + 5.4\,\alpha_s + \mathcal{O}(\alpha_s^2)\big]\,,\end{aligned}$$

$$\begin{aligned}&\sigma_{\ge 2}\big(p_{T1}^{\rm jet} \ge 30\,\text{GeV}, p_{T2}^{\rm jet} \ge 30\,\text{GeV}\big)\\ &\quad = (2.00\,\text{pb})\big[3.6\,\alpha_s + \mathcal{O}(\alpha_s^2)\big]\,.\end{aligned} \tag{20}$$

For $\sigma_1 = \sigma_{\ge 1} - \sigma_{\ge 2}$ there is a sizeable cancellation between these α_s terms. If we lower the cut to $p_{T2}^{\rm jet} \ge 22\,\text{GeV}$ then the logarithm increases and there is an almost exact cancellation with the $5.4\alpha_s$. In the top right panel of Fig. 1 we plot σ_1 as a function of $p_T^{\rm cut}$, and we again see that this cancellation occurs in a region where there is a dramatic decrease in the direct exclusive scale dependence (green dashed and dotted curves). Using the inclusive uncertainties for $\sigma_{\ge 1}$ and $\sigma_{\ge 2}$, and adding them in quadrature, gives the solid red curves, which again avoids this problem and provides a more realistic estimate for the perturbative uncertainty.

Using the result from App. A we can examine the full uncertainties and correlation matrix with 0, 1, and ($\ge$ 2)-jet bins in Higgs production. For the cuts in Eq. (20) varying the scale by factors of two, we have

$\sigma_{\rm total} = (8.70 \pm 0.75)\,{\rm pb}$, $\sigma_{\geq 1} = (3.29 \pm 0.62)\,{\rm pb}$, and $\sigma_{\geq 2} = (0.85 \pm 0.49)\,{\rm pb}$, corresponding to relative uncertainties of 8.6%, 18.8%, and 57%, respectively. We let $\delta(x)$ denote the relative percent uncertainty of the quantity x, and $\rho(x,y)$ the correlation coefficient between x and y. App. A yields

$$\begin{aligned} \delta(\sigma_0) &= 18\%\,, & \delta(\sigma_1) &= 32\%\,, \\ \rho(\sigma_0,\sigma_{\rm total}) &= 0.77\,, & \rho(\sigma_1,\sigma_{\geq 2}) &= -0.62\,, \\ \rho(\sigma_0,\sigma_1) &= -0.50\,, \end{aligned} \tag{21}$$

where we have only shown the nonzero correlations. Note that σ_0 and σ_1 as well as σ_1 and $\sigma_{\geq 2}$ have a substantial negative correlation because of the jet-bin boundary they share, while σ_0 and $\sigma_{\geq 2}$ are uncorrelated.

In contrast, the direct exclusive scale variation results in all the cross sections being 100% correlated. Due to the cancellations between the perturbative series, this leads to much smaller (and unrealistic) uncertainties, with our choice of cuts $\delta(\sigma_0) = 2.3\%$ and $\delta(\sigma_1) = 5.5\%$, which is reflected in the pinching of the green lines in Fig. 2. (Note that increasing the range of scale variation or separately varying μ_r and μ_f does not mitigate this problem.) The analog of Eq. (1) for this example would be

$$0.62 \times 2.3\% + 0.28 \times 5.5\% + 0.10 \times 57\% = 8.6\%\,. \tag{22}$$

When all σ_i are 100% correlated, σ_0 is forced to have a smaller relative uncertainty than $\sigma_{\rm total}$, as in Eq. (1), since it has to make up for the much larger uncertainties in $\sigma_{\geq 2}$.

In addition to the cross sections in each jet bin, we can also consider the relative jet fractions $f_0 = \sigma_0/\sigma_{\rm total}$ and $\sigma_1/\sigma_{\rm total}$, which are often used in experimental analyses. The perturbative theory uncertainties and correlations for the jet fractions follow by standard error propagation from those in Eq. (21). The general expressions are given in App. A, and we find

$$\begin{aligned} \delta(f_0) &= 13\%\,, & \delta(f_1) &= 33\%\,, \\ \rho(f_0,\sigma_{\rm total}) &= 0.42\,, & \rho(f_1,\sigma_{\rm total}) &= -0.26\,, \\ \rho(f_0,f_1) &= -0.80\,. \end{aligned} \tag{23}$$

Comparing to Eq. (21), the use of jet fractions with $\sigma_{\rm total}$ in the denominator yields a nonzero anti-correlation for $\sigma_{\rm total}$ with the 1-jet bin, and decreases the correlation for $\sigma_{\rm total}$ with the 0-jet bin.

It is also interesting to consider the case with $p_{T1}^{\rm jet} \geq 120\,{\rm GeV}$, where the logarithms of $p_{T1}^{\rm jet}/m_H$ are not large. The cross section $\sigma_{\geq 1}$ now has a smaller perturbative correction, but for a region of cuts on $p_{T2}^{\rm jet}$ there are still substantial cancellations in σ_1. For instance, for $p_{T2}^{\rm jet} \geq 60\,{\rm GeV}$ we have

$$\begin{aligned} &\sigma_{\geq 1}\big(p_{T1}^{\rm jet} \geq 120\,{\rm GeV}\big) \\ &\qquad = (0.31\,{\rm pb})\big[1 + 2.9\,\alpha_s + \mathcal{O}(\alpha_s^2)\big]\,, \\ &\sigma_{\geq 2}\big(p_{T1}^{\rm jet} \geq 120\,{\rm GeV}, p_{T2}^{\rm jet} \geq 60\,{\rm GeV}\big) \\ &\qquad = (0.31\,{\rm pb})\big[3.7\,\alpha_s + \mathcal{O}(\alpha_s^2)\big]\,, \end{aligned} \tag{24}$$

and the α_s terms completely cancel around $p_{T2}^{\rm jet} \geq 70\,{\rm GeV}$. In the bottom right panel of Fig. 1 we plot σ_1 as a function of $p_T^{\rm cut}$ for this scenario. Once again the combined inclusive uncertainties (solid red curves) give a better estimate than the direct exclusive scale uncertainty determined by up/down μ variation in σ_1 (green dotted and dashed curves). It is interesting to notice that the curves dive and a logarithmic summation in $p_{T2}^{\rm jet}$ becomes important earlier now, i.e., at much larger values for $p_{T2}^{\rm jet}$, when the cut on $p_{T1}^{\rm jet}$ is raised. For $p_{T1}^{\rm jet} \geq 120\,{\rm GeV}$ and $p_{T2}^{\rm jet} \leq 30\,{\rm GeV}$ fixed-order perturbation theory does not yield a controlled expansion, and the resummation of the jet-veto logarithms is clearly necessary.

C. $WW + 0$ Jets

The process $pp \to WW + 0$ jets is the dominant irreducible background for the $H \to WW^*$ search in the 0-jet bin, and also exhibits a relatively large K factor ~ 1.5. Hence, it is interesting to contrast the scale uncertainties here with those found for $H + 0$ jets. Including the Higgs search cuts (modulo the jet veto), the K factor for WW becomes larger than two [19], but we will not include those cuts in our analysis here. With $\mu_r = \mu_f = m_W$, NLO MSTW2008 PDFs, and $\alpha_s \equiv \alpha_s(m_W) = 0.1226$, the total $pp \to WW$ cross section is

$$\sigma_{\rm total} = (32.5\,{\rm pb})\big[1 + 3.6\,\alpha_s + \mathcal{O}(\alpha_s^2)\big]\,, \tag{25}$$

while for the inclusive 1-jet cross section with logarithms of $p_T^{\rm cut}$ we have

$$\sigma_{\geq 1}\big(p_T^{\rm jet} \geq 30\,{\rm GeV}\big) = (32.5\,{\rm pb})\big[2.8\,\alpha_s + \mathcal{O}(\alpha_s^2)\big]\,. \tag{26}$$

Thus, when we consider $\sigma_0 = \sigma_{\rm total} - \sigma_{\geq 1}$ there is a sizeable cancellation for the α_s terms. In Fig. 1, lower left panel, we show σ_0 for $pp \to WW + 0$ jets as a function of $p_T^{\rm cut}$. Once again the green curves from direct exclusive scale variation exhibit a pinching near $p_T^{\rm cut} \sim 30\,{\rm GeV}$ due to cancellations between the two perturbative series in Eqs. (25) and (26), leading to an underestimate of the perturbative uncertainty. The combined inclusive uncertainty estimate again mitigates this problem. The pattern of uncertainties here is the same as for $H + 0$ jets and $H + 1$ jet, just with smaller overall uncertainties. Just like for $H + 0$ jets using independent variations for μ_f and μ_r does not change the picture, the μ_f variation for fixed μ_r is again quite small.

D. $W + 0$ Jets

The exclusive process $pp \to W + N$ jets is an important benchmark process at the LHC and also an important SM background for new physics searches looking for

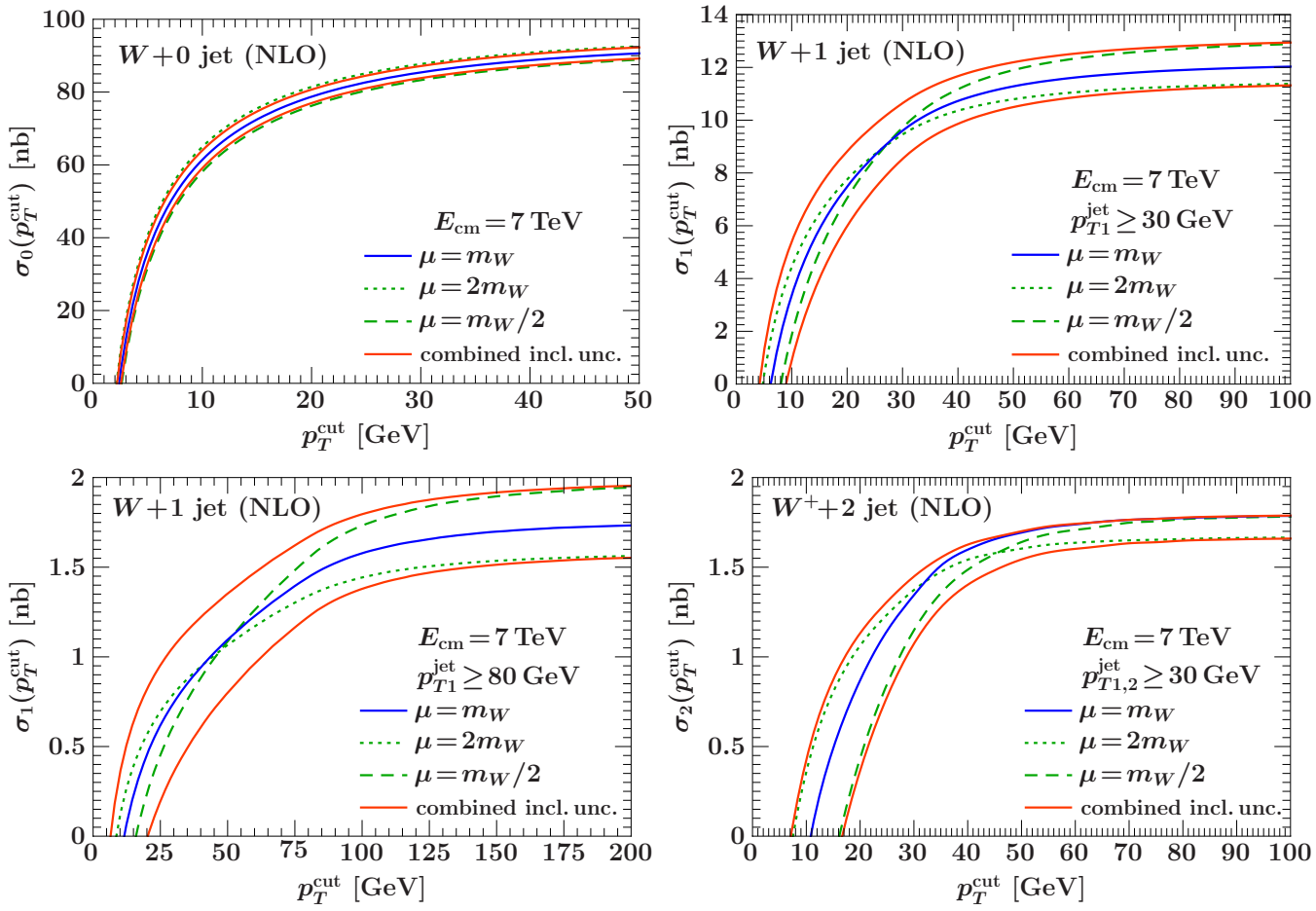

FIG. 3: Fixed-order perturbative uncertainties for the exclusive $pp \to W + 0, 1, 2$ jet cross sections at NLO for the LHC with $E_{\rm cm} = 7\,\text{TeV}$. Central values are shown by blue solid curves, direct exclusive scale variation in the exclusive jet bin by the green dashed and dotted curves, and the result of combining independent inclusive uncertainties to get the jet-bin uncertainty by the outer red solid curves.

missing energy. In this section we consider $pp \to W + 0$ jets, which provides us with a case to test our method when the perturbative corrections in the inclusive cross sections are not as large. For simplicity, we only work to NLO here. Using $\mu_f = \mu_r = m_W$ for the central value and MSTW2008 NLO PDFs, the inclusive W production cross section is

$$\sigma_{\rm total} = (80.7\,\text{nb})\big[1 + 1.3\,\alpha_s + \mathcal{O}(\alpha_s^2)\big]\,, \qquad (27)$$

where we have summed over $W^\pm$, and have not included the leptonic branching fractions. For the inclusive 1-jet cross section we have

$$\sigma_{\geq 1}\big(p_T^{\rm jet} \geq 30\,\text{GeV}\big) = (80.7\,\text{nb})\big[0.9\,\alpha_s + \mathcal{O}(\alpha_s^2)\big]\,. \quad (28)$$

The perturbative coefficients in Eqs. (27) and (28) are much smaller than in Higgs production. The resulting predictions for $\sigma_0(p_T^{\rm cut})$ are shown in the top left panel of Fig. 3, where the different lines have the same meaning as in Fig. 1. Since the α_s corrections are not very large here, the μ_f scale variation in the PDFs dominates over the μ_r variation in α_s and produces a 100% negative correlation between $\sigma_{\rm total}$ and $\sigma_{\geq 1}$. (Keeping μ_f fixed at m_W and only varying μ_r results in the expected pinching of the green lines.) This means their scale uncertainties add linearly in σ_0, which maximizes the uncertainty in this 0-jet cross section. In this case, our method, shown by the solid red lines, gives an uncertainty band very similar to direct exclusive scale variation. Hence, our method of using independent inclusive uncertainties still remains consistent for this situation.

E. $W + 1$ Jets

For $pp \to W + 1$ jet the perturbative corrections in $\sigma_{\geq 1}$ are larger than those in the W total cross section, which is in part influenced by logarithms from the lower cut on $p_{T1}^{\rm jet}$, the p_T of the leading jet. The situation for the $W+1$ jet bin is similar to $H + 1$ jet. Considering Eq. (19) the series for the inclusive 2-jet cross section, $\sigma_{\geq 2}$, has large double logarithms $L = \ln(p_{T2}^{\rm jet}/m_W)$ of the second largest

jet p_T, which are independent of those in the perturbative series for $\sigma_{\geq 1}$. Taking $\mu = m_W$ for central values, and using MSTW2008 PDFs at NLO, the total $W^+ + W^-$ cross sections with both jet cuts at 30 GeV are

$$\begin{aligned}
&\sigma_{\geq 1}\big(p_{T1}^{\text{jet}} \geq 30\,\text{GeV}\big) \\
&\qquad = (8.61\,\text{nb})\big[1 + 3.4\,\alpha_s + \mathcal{O}(\alpha_s^2)\big]\,, \\
&\sigma_{\geq 2}\big(p_{T1}^{\text{jet}} \geq 30\,\text{GeV}, p_{T2}^{\text{jet}} \geq 30\,\text{GeV}\big) \\
&\qquad = (8.61\,\text{nb})\big[2.5\,\alpha_s + \mathcal{O}(\alpha_s^2)\big]\,.
\end{aligned} \tag{29}$$

Once again the result for $\sigma_{\geq 2}$ and the precise cancellation that occurs in σ_1 is quite sensitive to p_T^{cut}, the cut on p_{T2}^{jet}, yielding an almost exact cancellation of the $3.4\,\alpha_s$ for $p_{T2}^{\text{jet}} \geq 25\,\text{GeV}$. In the top-right panel of Fig. 3 we plot σ_1 as a function of p_T^{cut}, with direct exclusive scale variation (green dashed and dotted curves) and those derived from independent inclusive uncertainties (solid red curves). Just like for $H+1$ jet, the direct exclusive scale variation curves pinch, while the inclusive curves avoid this problem and remain realistic.

We can also consider what happens when we make a larger cut on p_{T1}^{jet}. Here, unlike for Higgs, the relative size of the perturbative correction in $\sigma_{\geq 1}$ increases. For instance,

$$\begin{aligned}
&\sigma_{\geq 1}\big(p_{T1}^{\text{jet}} \geq 80\,\text{GeV}\big) \\
&\qquad = (1.07\,\text{nb})\big[1 + 5.3\,\alpha_s + \mathcal{O}(\alpha_s^2)\big]\,, \\
&\sigma_{\geq 2}\big(p_{T1}^{\text{jet}} \geq 80\,\text{GeV}, p_{T2}^{\text{jet}} \geq 60\,\text{GeV}\big) \\
&\qquad = (1.07\,\text{nb})\big[4.1\,\alpha_s + \mathcal{O}(\alpha_s^2)\big]\,.
\end{aligned} \tag{30}$$

For $p_{T2}^{\text{jet}} \geq p_T^{\text{cut}}$ in $\sigma_{\geq 2}$ the resulting 1-jet cross section σ_1 is shown as a function of p_T^{cut} in the bottom-left panel of Fig. 3. The situation for the uncertainties is similar to that for the less stringent cut on p_{T1}^{jet} in the upper-right panel. Much like in $H+1$ jet the logarithms start to influence the cross section at larger values of p_T^{cut} for the larger p_{T1}^{jet} cut.

F. $W + 2$ Jets

As our last example we consider $W + 2$ jets, and for simplicity we only consider the case of W^+ production. The inclusive 2-jet and 3-jet cross sections with all jets cut at 30 GeV are

$$\begin{aligned}
\sigma_{\geq 2}\big(p_{T1,2}^{\text{jet}} \geq 30\,\text{GeV}\big) &= (1.60\,\text{nb})\big[1 + 1.0\,\alpha_s + \mathcal{O}(\alpha_s^2)\big]\,, \\
\sigma_{\geq 3}\big(p_{T1,2,3}^{\text{jet}} \geq 30\,\text{GeV}\big) &= (1.60\,\text{nb})\big[2.3\,\alpha_s + \mathcal{O}(\alpha_s^2)\big]\,,
\end{aligned} \tag{31}$$

and the resulting exclusive 2-jet cross section as a function of the p_T^{cut} on the third jet is shown in the bottom-right panel in Fig. 3.

There are two different types of diagrams contributing to this process, those having two external quark lines and two gluon lines at lowest order ($qqgg$), and those having four external quark lines at lowest order ($qqqq$). The $qqgg$-type contributions have the same behavior as $W + 1$ jet, again displaying a pinching in the direct exclusive scale variation curves. On the other hand, in the $qqqq$-type contributions the PDF scale dependence dominates, similar to what we observed for $W + 0$ jets. The combination of the two leads to the behavior seen in Fig. 3 at large p_T^{cut}, where the scale uncertainties in the inclusive 2-jet cross section are asymmetric. Here there is some choice for how to combine the scale variation into an uncertainty estimate for $\sigma_{\geq 2}$ (green dashed and dotted curves). The choice one makes for $\sigma_{\geq 2}$ simply propagates into the equivalent choice for the exclusive 2-jet bin σ_2 (solid red curves). For simplicity in the bottom-right panel of Fig. 3 we still use $\mu = m_W/2$ and $\mu = 2m_W$ to determine $\Delta_{\geq 2}$, in which case the central value should be taken as the center of the band rather than the blue line for $\mu = m_W$.

For $W+2$ jets in Fig. 3 the pinching caused by the $qqgg$ contributions is again mitigated by combining the inclusive uncertainties. Hence, we see that our method can be applied and gives more stable uncertainty estimates even in more complicated cases where several components contribute to the cross section.

Note that we have also checked that when increasing the cuts on the two leading jets, the same effect as in $H+1$ jets and $W + 1$ jets happens here as well. Namely, the jet-veto logarithms from restricting the third jet become more important earlier and influence the cross section at larger values of p_T^{cut} for larger $p_{T1,2}^{\text{jet}}$ cuts.

IV. RESUMMATION FOR HIGGS + 0 JETS

In Sec. III we have seen that direct exclusive scale variation often leads to an accidental underestimate of the uncertainties for exclusive jet bin cross sections for a range of experimentally relevant cuts. Instead combining independent uncertainties on inclusive cross sections yields a more uniform (and larger) uncertainty band for the exclusive jet bins. The region where direct exclusive scale variation runs into trouble borders the region where the resummation of the large logarithms of p_T^{jet} becomes important. In this section, we test how realistic the fixed-order scale uncertainties are by comparing them to a case where the resummation of large logarithms induced by the jet bin are known to NNLL+NNLO accuracy.

We again consider $H + 0$ jets from gluon fusion. At NNLL order accuracy the resummation is sensitive to the precise jet algorithm used to define p_T^{jet}, and other complications in the required theoretical setup. To avoid these issues, we will use a slightly different variable to define the 0-jet bin, an inclusive event shape known as beam thrust [34],

$$\mathcal{T}_{\text{cm}} = \sum_k (E_k - |p_k^z|)\,. \tag{32}$$

The sum over k runs over all particles except the Higgs

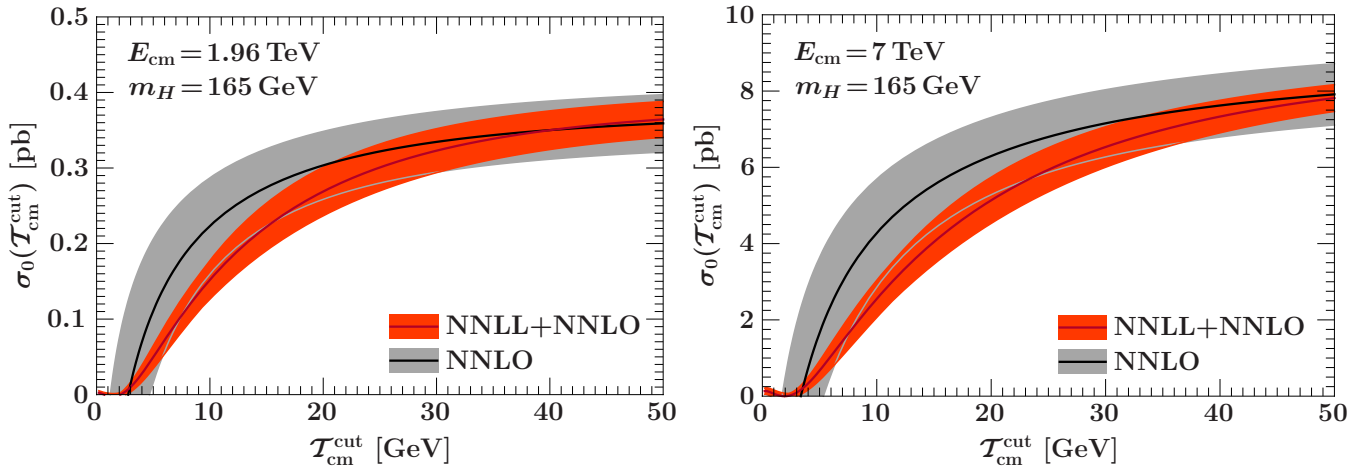

FIG. 4: Comparison of $gg \to H + 0$ jets using $\mathcal{T}_{\rm cm}^{\rm cut}$ at fixed NNLO with the resummed results at NNLL+NNLO. For the fixed-order uncertainties in σ_0 we use independent inclusive scale variations in $\sigma_{\rm total}$ and $\sigma_{\geq 1}$. The uncertainty method for the resummed results is described in the text.

decay products. Beam thrust essentially measures the thrust of an event along the $\hat{z}$ beam axis. When $\mathcal{T}_{\rm cm} \leq \mathcal{T}_{\rm cm}^{\rm cut}$, from Eq. (32) we see that events in $\sigma_0(\mathcal{T}_{\rm cm})$ are only allowed to contain hard radiation in the forward regions at large rapidities, and hence this cut vetoes central jets. Much like with $p_T^{\rm jet}$ the perturbative series for this σ_0 has double logarithms, for example the analog of Eq. (7) is

$$\sigma_0(\mathcal{T}_{\rm cm}^{\rm cut}) = \sigma_B\Big(1 - \frac{3\alpha_s}{\pi}\,\ln^2\frac{\mathcal{T}_{\rm cm}^{\rm cut}}{m_H} + \cdots\Big)\,. \qquad (33)$$

For beam thrust, the all-order resummation of perturbative corrections is known to NNLL order for both $H + 0$ jets and $V + 0$ jets [35–37]. For Higgs production the computation has been extended to fully include all NNLO corrections, and it was observed that the resummed cross section at NNLL+NNLO had larger uncertainties than the pure NNLO result for $\sigma_0(\mathcal{T}_{\rm cm} \leq \mathcal{T}_{\rm cm}^{\rm cut})$ utilizing direct exclusive fixed-order scale variation. This lead to the conclusion that the direct exclusive scale variation underestimates the fixed-order perturbative uncertainties in the 0-jet bin. In the resummed calculation, fixed-order α_s expansions are carried out at three distinct scales (hard μ_H, jet/beam μ_B, and soft μ_S) which appear in the corresponding factorization theorem. The uncertainties in the resummed cross section are obtained by varying these scales. Varying μ_H up and down by a factor of two moves all three scales up and down, and hence is a scale variation that is correlated with the usual scale variation for the inclusive cross section. Varying μ_B or μ_S while holding μ_H fixed explicitly accounts for additional higher order uncertainties induced by the presence of the large jet-veto logarithms, and hence allow us to determine $\Delta_{\rm cut}$.

In Fig. 4 we compare the remaining perturbative uncertainties after resummation at NNLL+NNLO, shown by the darker orange bands, to the NNLO uncertainties obtained with the fixed-order method advocated here, which are shown by the lighter gray bands. The results for the NNLL+NNLO cross section are obtained from Ref. [37].[5] The left panel shows the results for the Tevatron and the right panel the results for the LHC at 7 TeV. The fact that the resummation reduces the perturbative uncertainties, as it should, shows that our method of using independent inclusive scale variations yields more robust fixed-order uncertainties.

In the resummed calculation, $\sigma_{\rm total}$ is by construction not affected by the μ_S and μ_B variations. We denote the combined μ_S and μ_B uncertainty by Δ_{SB}. It provides a direct estimate of the cut-induced uncertainty, $\Delta_{\rm cut} = \Delta_{SB}$, which is anti-correlated between $\sigma_0(\mathcal{T}_{\rm cm}^{\rm cut})$ and the corresponding $\sigma_{\geq 1}(\mathcal{T}_{\rm cm}^{\rm cut}) = \sigma_{\rm total} - \sigma_0(\mathcal{T}_{\rm cm}^{\rm cut})$. On the other hand, the μ_H variation affects all the cross sections yielding an uncertainty component that is 100% correlated between them. In particular, it is responsible for estimating the perturbative uncertainty of $\sigma_{\rm total}$, for which it is equivalent to the usual fixed-order scale variation, $\Delta_{H\rm tot} = \Delta_{\rm total}$. The full covariance matrix for $\{\sigma_{\rm total}, \sigma_0, \sigma_{\geq 1}\}$, that is the analog of Eq. (12) but for

[5] We have made a small improvement to Ref. [37]. The NNLL+NNLO results of Ref. [37] fully incorporate the NNLO corrections by adding so-called nonsingular fixed-order contributions, which are terms that do not appear in an expansion of the strict NNLL result. In Ref. [37] the nonsingular contributions were obtained for the sum of $\mathcal{O}(\alpha_s) + \mathcal{O}(\alpha_s^2)$ cross-sections using FEHiP [30, 31]. Here we use a much higher statistics spectrum from MCFM [17], which allows us to separately determine the nonsingular cross sections at $\mathcal{O}(\alpha_s)$ and $\mathcal{O}(\alpha_s^2)$. The only place this improvement is visible is for $\mathcal{T}_{\rm cm}^{\rm cut} \leq 3\,\text{GeV}$, where the resummed cross sections are now consistent with zero within the displayed uncertainties.

the resummed result, is then

$$C = C_{SB} + C_H\,,$$
$$C_{SB} = \begin{pmatrix} 0 & 0 & 0 \\ 0 & \Delta_{SB}^2 & -\Delta_{SB}^2 \\ 0 & -\Delta_{SB}^2 & \Delta_{SB}^2 \end{pmatrix}, \tag{34}$$
$$C_H = \begin{pmatrix} \Delta_{H\mathrm{tot}}^2 & \Delta_{H\mathrm{tot}}\Delta_{H0} & \Delta_{H\mathrm{tot}}\,\Delta_{H\geq 1} \\ \Delta_{H\mathrm{tot}}\,\Delta_{H0} & \Delta_{H0}^2 & \Delta_{H0}\,\Delta_{H\geq 1} \\ \Delta_{H\mathrm{tot}}\,\Delta_{H\geq 1} & \Delta_{H0}\,\Delta_{H\geq 1} & \Delta_{H\geq 1}^2 \end{pmatrix},$$

where Δ_{SB} is obtained from the envelope of the μ_S and μ_B variations, and C_{SB} is equivalent to C_{cut} in Eq. (6). The Δ_{Hi} are obtained from the μ_H variation and satisfy $\Delta_{H\mathrm{tot}} = \Delta_{H0} + \Delta_{H\geq 1}$. The full uncertainty in the 0-jet bin shown by the darker red bands in Fig. 4 is then given by $\Delta_{SB}^2 + \Delta_{H0}^2$, which is the 0-bin entry on the diagonal of C.[6]

Compared to Eq. (34), using a direct exclusive scale variation at fixed order would correspond to taking $\Delta_{SB} \to 0$ and obtaining the analog of the Δ_{Hi} by scale variation without resummation ($\mu_H = \mu_B = \mu_S$). On the other hand, our proposed fixed-order method would correspond to taking $\Delta_{SB} \to \Delta_{\geq 1}$ and $\Delta_{H\geq 1} \to 0$, such that $\Delta_{H0} = \Delta_{H\mathrm{tot}} \to \Delta_{\mathrm{total}}$. Hence, the resummation of the jet-veto logarithms allows one to capture both types of uncertainties appearing in the two different fixed-order methods. Note that the numerical dominance of Δ_{SB}^2 over $\Delta_{H0}\Delta_{H\geq 1}$ in the 0-jet region is another way to justify the preference for using the combined inclusive scale variation over the direct exclusive scale variation when given a choice between these two methods.

As an example, consider $\mathcal{T}_{\mathrm{cm}}^{\mathrm{cut}} = 20\,\mathrm{GeV}$. At fixed NNLO, the inclusive cross sections are $\sigma_{\mathrm{total}} = (8.70 \pm 0.75)\,\mathrm{pb}$ and $\sigma_{\geq 1} = (2.25 \pm 0.62)\,\mathrm{pb}$. Using Eq. (12), this gives

$$\begin{aligned} \delta(\sigma_0) &= 15\%\,, & \delta(\sigma_{\geq 1}) &= 28\%\,, \\ \rho(\sigma_0, \sigma_{\mathrm{total}}) &= 0.77\,, & \rho(\sigma_{\geq 1}, \sigma_{\mathrm{total}}) &= 0\,, \\ \rho(\sigma_0, \sigma_{\geq 1}) &= -0.64\,. \end{aligned} \tag{35}$$

For σ_0 this corresponds to the gray bands in Fig. 4, and the structure here is very similar to what we saw in Eq. (21).

From our resummed result using Eq. (34) we obtain

$$\begin{aligned} \delta(\sigma_0) &= 11.8\%\,, & \delta(\sigma_{\geq 1}) &= 19.7\%\,, \\ \rho(\sigma_0, \sigma_{\mathrm{total}}) &= 0.04\,, & \rho(\sigma_{\geq 1}, \sigma_{\mathrm{total}}) &= 0.33\,, \\ \rho(\sigma_0, \sigma_{\geq 1}) &= -0.82\,, \end{aligned} \tag{36}$$

which for σ_0 corresponds to the orange bands in Fig. 4. After resummation neither of σ_0 and $\sigma_{\geq 1}$ is strongly correlated with σ_{total} anymore, which at first sight is perhaps a bit surprising. However, for small $\mathcal{T}_{\mathrm{cm}}^{\mathrm{cut}}$ this is not unexpected and is simply due to the fact that the central values and remaining perturbative uncertainties are dominated by the resummed logarithmic series (i.e. Δ_{SB} dominates numerically over Δ_{H0} and $\Delta_{H\geq 1}$). In fact, this supports our arguments in Sec. II, that the uncertainties from higher-order terms in the logarithmic series for $\sigma_{\geq 1}$ and the fixed-order series for σ_{total} can and should be considered independent, which lead to Eq. (11).

Comparing Eqs. (35) and (36), we see that the uncertainties obtained from our fixed-order method follow a similar pattern for the relative uncertainties for σ_0 and $\sigma_{\geq 1}$ as observed in the resummed result, with a strong negative correlation between them. Since resummation provides an improved treatment of the cut-induced effects, we take this as further evidence that the method of using inclusive fixed-order cross section uncertainties provides a consistent way to obtain reliable estimates of perturbative uncertainties in exclusive jet bins. In particular it provides a suitable starting point for an uncertainty estimate, that can be further refined when an appropriate resummed result becomes available.

V. CONCLUSIONS

We have proposed a method to estimate perturbative uncertainties in fixed-order predictions of exclusive jet cross sections that accounts for the presence of large logarithms at higher orders caused by the jet binning. The method uses the fixed-order calculations of inclusive cross sections, $\sigma_{\geq N}$ and $\sigma_{\geq N+1}$, for which the standard scale variation provides reasonable uncertainty estimates, and combines these inclusive uncertainties into an estimate for the corresponding exclusive N-jet cross section $\sigma_N = \sigma_{\geq N} - \sigma_{\geq N+1}$, treating the inclusive cross sections as uncorrelated.

We have illustrated this procedure for a variety of processes, including analysis of $H + 0, 1$ jets, $WW + 0$ jets, and $W + 0, 1, 2$ jets with MCFM, and showed that it yields more robust estimates of theory uncertainties than direct exclusive scale variation. We have also shown for a specific case with $H + 0$ jets that it leads to fixed-order uncertainties that are theoretically consistent with the corresponding resummed predictions. In jet bins used for new physics searches, we anticipate that it should yield realistic uncertainty estimates for standard model backgrounds. We also expect that it provides a suitable fixed-order starting point for the central values, uncertainties, and jet bin correlations, which can be improved by higher-order logarithmic resummation.

Our treatment of the fixed-order exclusive and inclusive cross sections has followed the standard approach of always using cross section results at the same order in α_s. It would be interesting to study whether this can be

[6] In the results of Ref. [37], the envelope of all three scale variations was used to obtain the total uncertainty. The slightly modified procedure we use here, which adds Δ_{SB} and Δ_H in quadrature, gives very similar results, but has the advantage that it also allows for a straightforward treatment of the correlations.

relaxed when using differences of inclusive cross sections to compute the central values for the jet bins. For example, for $gg \to H$ one could independently compute $\sigma_{\rm total}$ at NNLO, and $\sigma_{\geq 1}$ and $\sigma_{\geq 2}$ each at NLO, and then use these to compute the jet bins as $\sigma_0 = \sigma_{\rm total} - \sigma_{\geq 1}$ and $\sigma_1 = \sigma_{\geq 1} - \sigma_{\geq 2}$. Since we argued that the inclusive series can be treated independently, it may be consistent to include them to different orders to compute the central value and uncertainties of σ_1. This would have the advantage of allowing one to utilize the NLO result for $\sigma_{\geq 2}$ without destroying the consistent perturbative expansion for $\sigma_{\geq 1}$ and $\sigma_{\rm total}$ when the jet bins are added together. Since in this case the perturbative order of the jet boundary between σ_1 and $\sigma_{\geq 2}$ does not match up, this deserves a dedicated study before being used in practice.

Acknowledgments

We thank the organizers and participants of the workshop "Higgs at Tevatron and LHC" for stimulating discussion which inspired this work. The workshop was sponsored by the University of Washington and supported by the DOE under contract DE-FGO2-96-ER40956. We thank Joey Huston, Frank Petriello and Massimiliano Grazzini for stimulating discussions and comments on the manuscript. Parts of this work have been carried out within the LHC Higgs Cross Section Working Group. This work was supported in part by the Office of Nuclear Physics of the U.S. Department of Energy under the grant DE-FG02-94ER40818, and by the Department of Energy under the grant DE-SC003916.

Appendix A: Case of Three Jet Bins

In this appendix we generalize Eq. (12) to the case of 0, 1, and (≥ 2)-jet bins that is actually used in current Higgs searches. Since only neighboring jet bins will be correlated, the generalization to more than three jet bins is not any more complicated.

We start from the inclusive cross sections $\sigma_{\rm total}$, $\sigma_{\geq 1}$, $\sigma_{\geq 2}$, and denote their absolute uncertainties by $\Delta_{\rm total}$, $\Delta_{\geq 1}$, $\Delta_{\geq 2}$ and their relative uncertainties by $\delta_i = \Delta_i/\sigma_i$. We define the exclusive cross sections and event fractions

$$\begin{aligned} \sigma_0 &= \sigma_{\rm total} - \sigma_{\geq 1}\,, & f_0 &= \frac{\sigma_0}{\sigma_{\rm total}}\,, \\ \sigma_1 &= \sigma_{\geq 1} - \sigma_{\geq 2}\,, & f_1 &= \frac{\sigma_1}{\sigma_{\rm total}}\,. \end{aligned} \tag{A1}$$

The covariance matrix for the four quantities $\{\sigma_{\rm total}, \sigma_0, \sigma_1, \sigma_{\geq 2}\}$ is given by

$$C = \begin{pmatrix} \Delta^2_{\rm total} & \Delta^2_{\rm total} & 0 & 0 \\ \Delta^2_{\rm total} & \Delta^2_{\rm total} + \Delta^2_{\geq 1} & -\Delta^2_{\geq 1} & 0 \\ 0 & -\Delta^2_{\geq 1} & \Delta^2_{\geq 1} + \Delta^2_{\geq 2} & -\Delta^2_{\geq 2} \\ 0 & 0 & -\Delta^2_{\geq 2} & \Delta^2_{\geq 2} \end{pmatrix}. \tag{A2}$$

Of course, only three of these four quantities are independent. For example, $\sigma_{\rm total} = \sigma_0 + \sigma_1 + \sigma_{\geq 2}$, and it is easy to check that $\Delta(\sigma_0 + \sigma_1 + \sigma_{\geq 2})^2 = \Delta^2_{\rm total}$, which is given by the sum of all entries in the lower 3×3 matrix. The relative uncertainties of $\sigma_{0,1}$ following from Eq. (A2), written in terms of relative quantities, are

$$\begin{aligned} \delta(\sigma_0)^2 &= \frac{1}{f_0^2}\,\delta^2_{\rm total} + \Big(\frac{1}{f_0} - 1\Big)^2 \delta^2_{\geq 1}\,, \\ \delta(\sigma_1)^2 &= \Big(\frac{1-f_0}{f_1}\Big)^2 \delta^2_{\geq 1} + \Big(\frac{1-f_0}{f_1} - 1\Big)^2 \delta^2_{\geq 2}\,. \end{aligned} \tag{A3}$$

Similarly, the correlation coefficients for σ_0 and σ_1 following from Eq. (A2) are

$$\begin{aligned} \rho(\sigma_0, \sigma_{\rm total}) &= \left[1 + \frac{\delta^2_{\geq 1}}{\delta^2_{\rm total}}(1-f_0)^2\right]^{-1/2}, \\ \rho(\sigma_0, \sigma_1) &= -\left[1 + \frac{\delta^2_{\rm total}}{\delta^2_{\geq 1}}\,\frac{1}{(1-f_0)^2}\right]^{-1/2} \\ &\quad \times \left[1 + \frac{\delta^2_{\geq 2}}{\delta^2_{\geq 1}}\Big(1 - \frac{f_1}{1-f_0}\Big)^2\right]^{-1/2}, \\ \rho(\sigma_0, \sigma_{\geq 2}) &= 0\,, \\ \rho(\sigma_1, \sigma_{\rm total}) &= 0\,, \\ \rho(\sigma_1, \sigma_{\geq 2}) &= -\left[1 + \frac{\delta^2_{\geq 1}}{\delta^2_{\geq 2}}\Big(1 - \frac{f_1}{1-f_0}\Big)^{-2}\right]^{-1/2}. \end{aligned} \tag{A4}$$

The relative uncertainties for f_0 and f_1 are

$$\begin{aligned} \delta(f_0)^2 &= \Big(\frac{1}{f_0} - 1\Big)^2 \big(\delta^2_{\rm total} + \delta^2_{\geq 1}\big)\,, \\ \delta(f_1)^2 &= \delta^2_{\rm total} + \Big(\frac{1-f_0}{f_1}\Big)^2 \delta^2_{\geq 1} + \Big(\frac{1-f_0}{f_1} - 1\Big)^2 \delta^2_{\geq 2}\,, \end{aligned} \tag{A5}$$

and their correlations are

$$\begin{aligned} \rho(f_0, \sigma_{\rm total}) &= \left[1 + \frac{\delta^2_{\geq 1}}{\delta^2_{\rm total}}\right]^{-1/2}, \\ \rho(f_0, f_1) &= -\left(1 + \frac{1-f_0}{f_1}\,\frac{\delta^2_{\geq 1}}{\delta^2_{\rm total}}\right)\Big(\frac{1}{f_0} - 1\Big)\,\frac{\delta^2_{\rm total}}{\delta(f_0)\delta(f_1)}\,, \\ \rho(f_1, \sigma_{\rm total}) &= -\frac{\delta_{\rm total}}{\delta(f_1)}\,. \end{aligned} \tag{A6}$$

[1] CDF and D0 Collaboration, T. Aaltonen *et al.*, Phys. Rev. Lett. **104**, 061802 (2010), [arXiv:1001.4162].
[2] CDF and D0 Collaboration, T. Aaltonen *et al.*, arXiv:1103.3233.
[3] CMS Collaboration, S. Chatrchyan *et al.*, Phys. Lett. B **699**, 25 (2011), [arXiv:1102.5429].
[4] ATLAS Collaboration, arXiv:1104.5225.
[5] B. Mellado, W. Quayle, and S. L. Wu, Phys. Lett. B **611**, 60 (2005), [hep-ph/0406095].
[6] B. Mellado, W. Quayle, and S. L. Wu, Phys. Rev. D **76**, 093007 (2007), [arXiv:0708.2507].
[7] The ATLAS Collaboration, G. Aad *et al.*, arXiv:0901.0512.
[8] C. Anastasiou, G. Dissertori, M. Grazzini, F. Stöckli, and B. R. Webber, JHEP **08**, 099 (2009), [arXiv:0905.3529].
[9] J. Baglio and A. Djouadi, JHEP **10**, 064 (2010), [arXiv:1003.4266].
[10] S. Alekhin, J. Blumlein, P. Jimenez-Delgado, S. Moch, and E. Reya, Phys. Lett. B **697**, 127 (2011), [arXiv:1011.6259].
[11] LHC Higgs Cross Section Working Group Collaboration, S. Dittmaier *et al.*, arXiv:1101.0593.
[12] J. Baglio, A. Djouadi, S. Ferrag, and R. M. Godbole, Phys. Lett. B **699**, 368 (2011), [arXiv:1101.1832].
[13] S. Alekhin, J. Blumlein, and S. Moch, arXiv:1101.5261.
[14] G. Watt, arXiv:1106.5788.
[15] R. S. Thorne and G. Watt, arXiv:1106.5789.
[16] J. Baglio, A. Djouadi, and R. Godbole, arxiv:1107.0281.
[17] J. M. Campbell and R. K. Ellis, Phys. Rev. D **60**, 113006 (1999), [hep-ph/9905386].
[18] J. M. Campbell and R. K. Ellis, Phys. Rev. D **65**, 113007 (2002), [hep-ph/0202176].
[19] J. M. Campbell, R. K. Ellis, and C. Williams, arXiv:1105.0020.
[20] J. M. Campbell, R. K. Ellis, and C. Williams, Phys. Rev. D **81**, 074023 (2010), [arXiv:1001.4495].
[21] S. Dawson, Nucl. Phys. B **359**, 283 (1991).
[22] A. Djouadi, M. Spira, and P. M. Zerwas, Phys. Lett. B **264**, 440 (1991).
[23] M. Spira, A. Djouadi, D. Graudenz, and P. M. Zerwas, Nucl. Phys. B **453**, 17 (1995), [hep-ph/9504378].
[24] R. V. Harlander and W. B. Kilgore, Phys. Rev. Lett. **88**, 201801 (2002), [hep-ph/0201206].
[25] C. Anastasiou and K. Melnikov, Nucl. Phys. B **646**, 220 (2002), [hep-ph/0207004].
[26] V. Ravindran, J. Smith, and W. L. van Neerven, Nucl. Phys. B **665**, 325 (2003), [hep-ph/0302135].
[27] A. Pak, M. Rogal, and M. Steinhauser, JHEP **02**, 025 (2010), [arXiv:0911.4662].
[28] R. V. Harlander, H. Mantler, S. Marzani, and K. J. Ozeren, Eur. Phys. J. C **66**, 359 (2010), [arXiv:0912.2104].
[29] A. D. Martin, W. J. Stirling, R. S. Thorne, and G. Watt, Eur. Phys. J. C **63**, 189 (2009), [arXiv:0901.0002].
[30] C. Anastasiou, K. Melnikov, and F. Petriello, Phys. Rev. Lett. **93**, 262002 (2004), [hep-ph/0409088].
[31] C. Anastasiou, K. Melnikov, and F. Petriello, Nucl. Phys. B **724**, 197 (2005), [hep-ph/0501130].
[32] S. Catani and M. Grazzini, Phys. Rev. Lett. **98**, 222002 (2007), [hep-ph/0703012].
[33] M. Grazzini, JHEP **02**, 043 (2008), [arXiv:0801.3232].
[34] I. W. Stewart, F. J. Tackmann, and W. J. Waalewijn, Phys. Rev. D **81**, 094035 (2010), [arXiv:0910.0467].
[35] I. W. Stewart, F. J. Tackmann, and W. J. Waalewijn, JHEP **09**, 005 (2010), [arXiv:1002.2213].
[36] I. W. Stewart, F. J. Tackmann, and W. J. Waalewijn, Phys. Rev. Lett. **106**, 032001 (2011), [arXiv:1005.4060].
[37] C. F. Berger, C. Marcantonini, I. W. Stewart, F. J. Tackmann, and W. J. Waalewijn, JHEP **04**, 092 (2011), [arXiv:1012.4480].